Article: Reconsidering initial Pb in titanite in the context of in situ dating
Journal Name: American Mineralogist
Authors: Chloë E. Bonamici & Tyler Blum
Corresponding Author E-mail: bonamici@wisc.edu
Address: Department of Geoscience, University of Wisconsin-Madison, 1215 W. Dayton St., Madison, WI, 53706, United States

Supplemental Materials

Supplemental Information: Reference materials performance during U-Pb analysis

Supplemental Text: Details of Tera-Wasserburg diagram model for Harrisville titanite

Figures S1-S13: Harrisville titanite grain images and U-Th-Pb traverse data

Table S1: SHRIMP U-Th-Pb titanite data for Harrisville samples

Table S2: LA-ICP-MS U-Th-Pb titanite data for Harrisville samples

Table S3: Semi-total Pb/U (2D) isochron regressions of U-Pb titanite data and associated goodness of fit metrics

Table S4. Total Pb/U (3D) isochron regressions of U-Pb titanite data and associated goodness-of-fit metrics.

American Mineralogist: November 2020 Deposit AM-20-117274

Supplemental Information

Reference materials performance during U-Pb analysis

LA-ICP-MS in-mount reference materials

The plots below show the weighted average 207-corrected $^{206}Pb/^{238}U$ dates and associated statistics for LA-ICM-MS analyses of reference materials. These provide an indication of the overall quality of the analytical method and data reduction (207-correction) applied to Adirondack titanite.

09HA03A in-mount BLR titanite std (accepted age: 1047.1 ± 0.4 Ma)

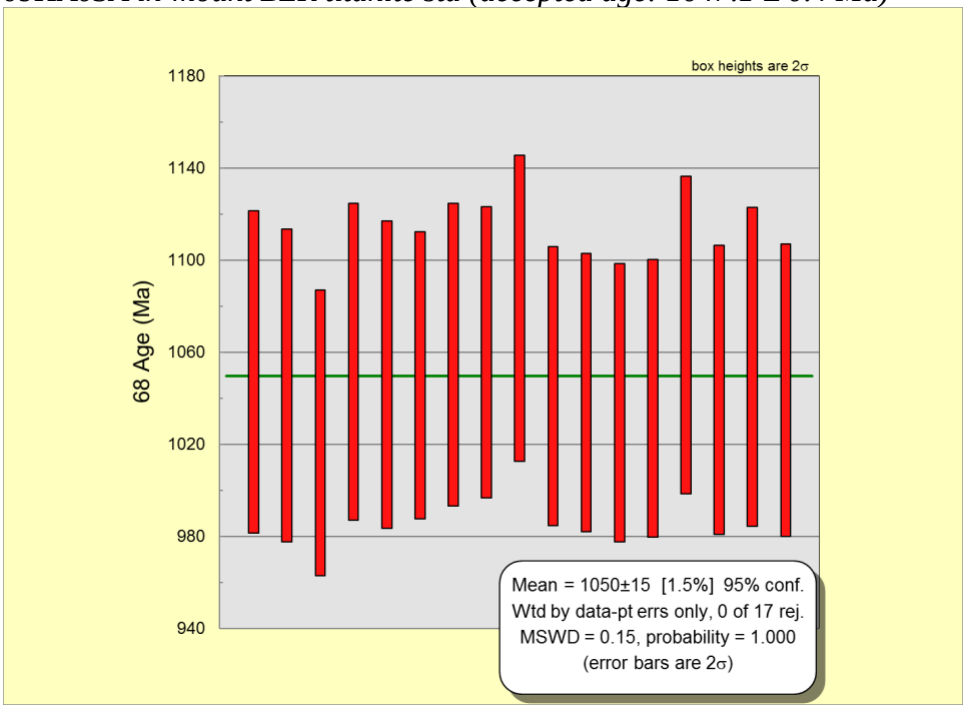

09HA03 in-mount Ecstall West zircon (accepted age: 91.5 ± 1.0 Ma)

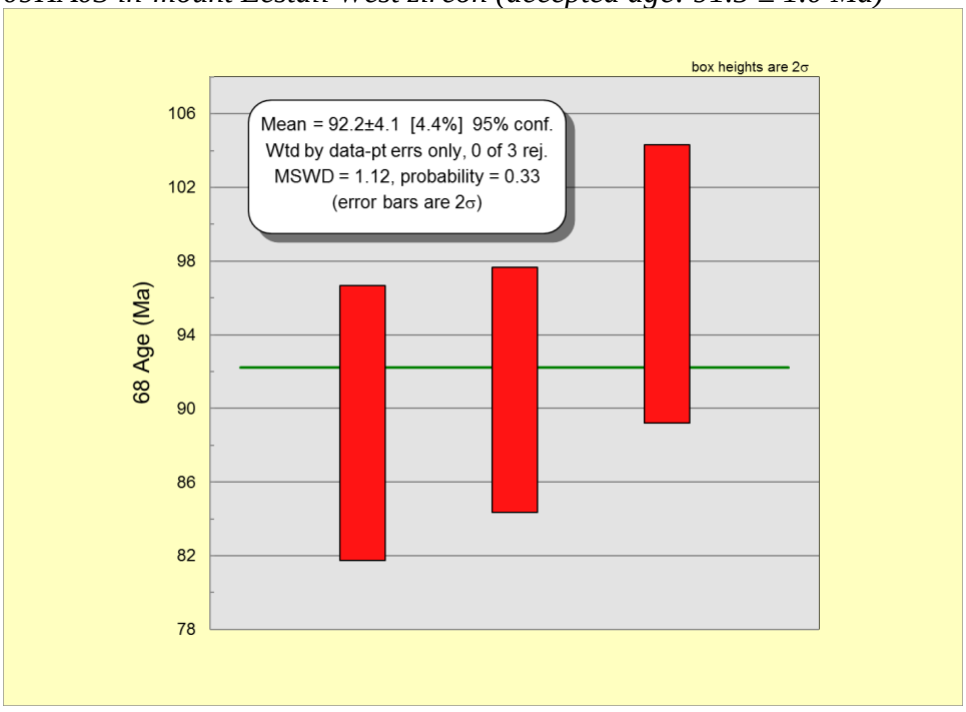

09HA07B in-mount BLR titanite std (accepted age: 1047.1 ± 0.4 Ma)

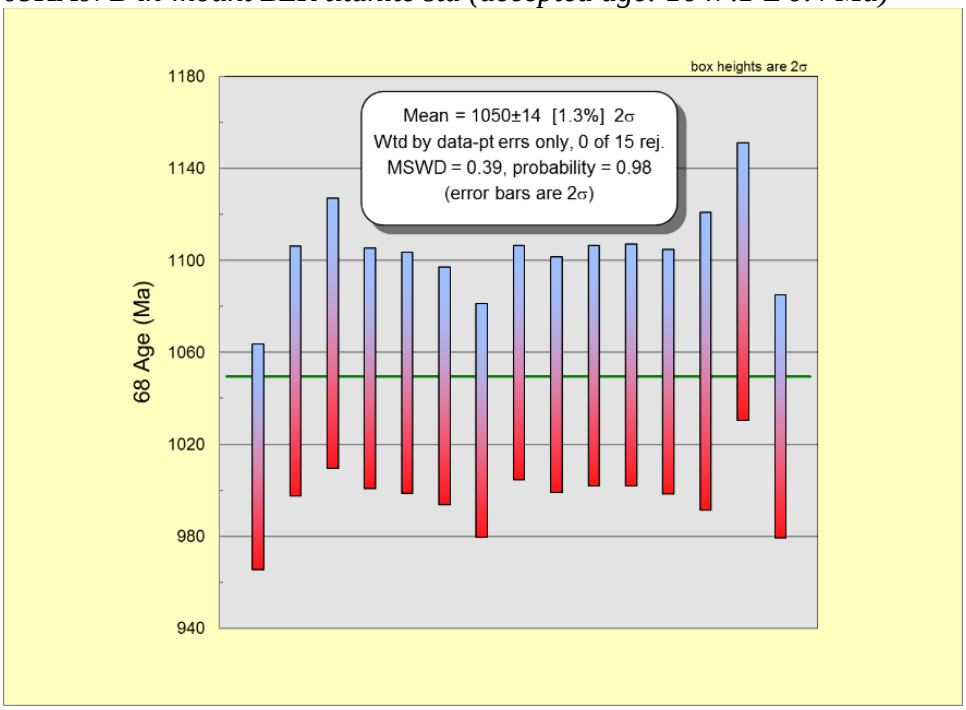

09HA07B in-mount Ecstall West zircon (accepted age: 91.5 ± 1.0 Ma)

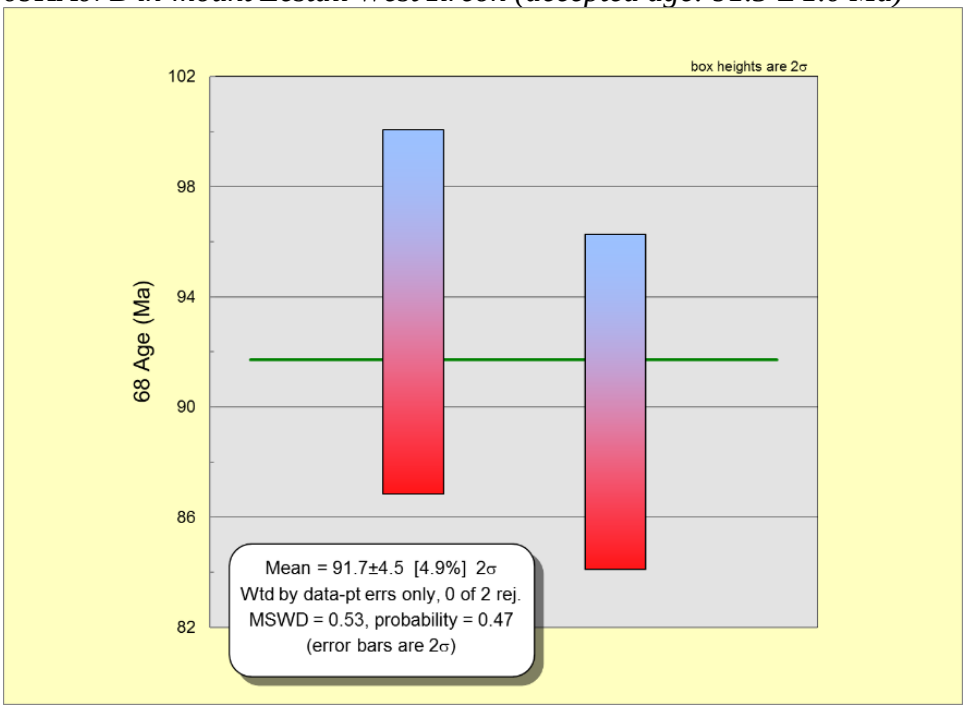

09HA08A in-mount BLR titanite std (accepted age: 1047.1 ± 0.4 Ma)

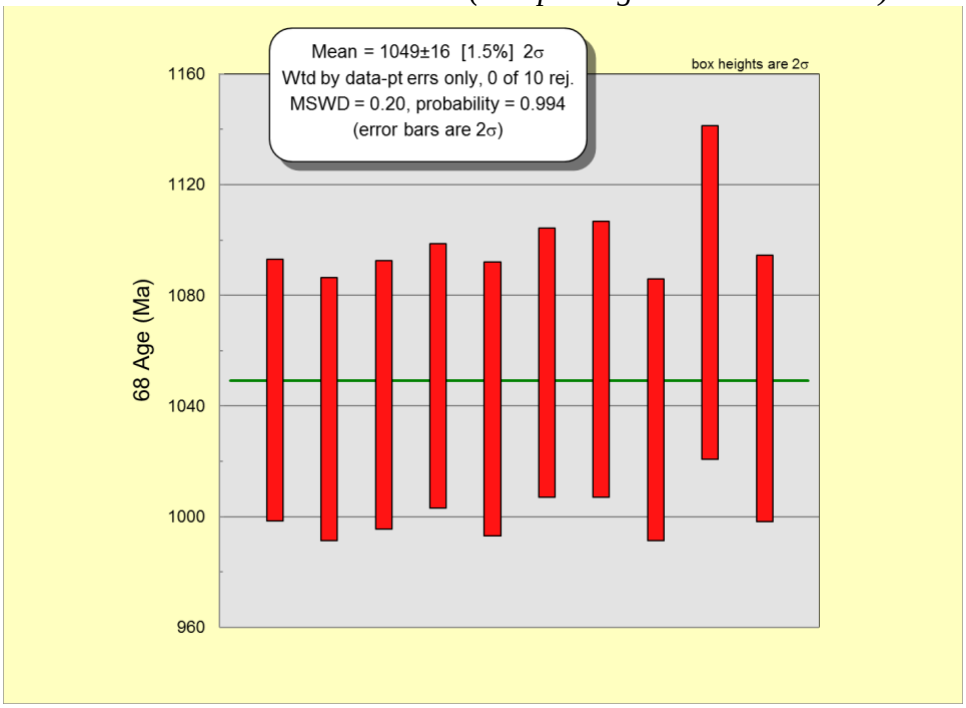

09HA08A in-mount Ecstall West zircon (accepted age: 91.5 ± 1.0 Ma)

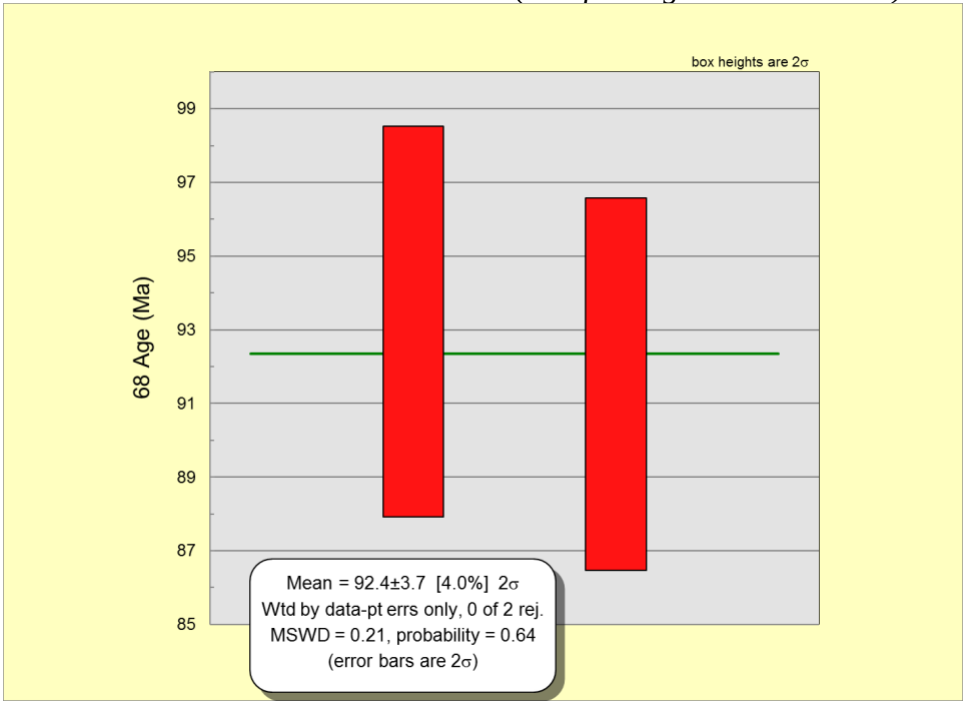

09HA09A in-mount BLR titanite std (accepted age: 1047.1 ± 0.4 Ma)

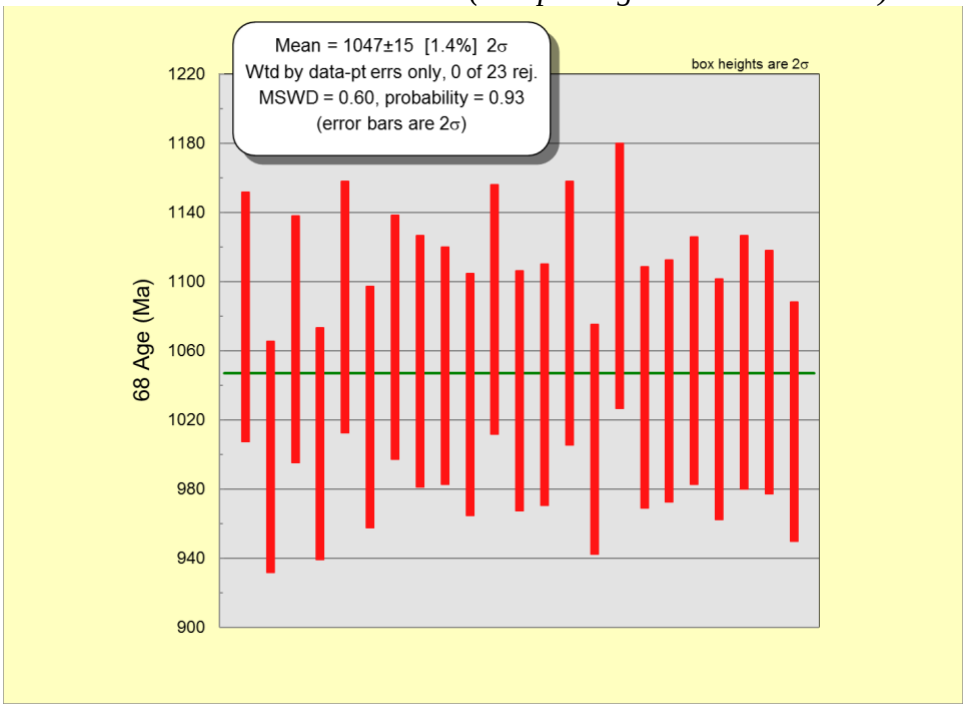

09HA09A in-mount Ecstall West zircon (accepted age: 91.5 ± 1.0 Ma)

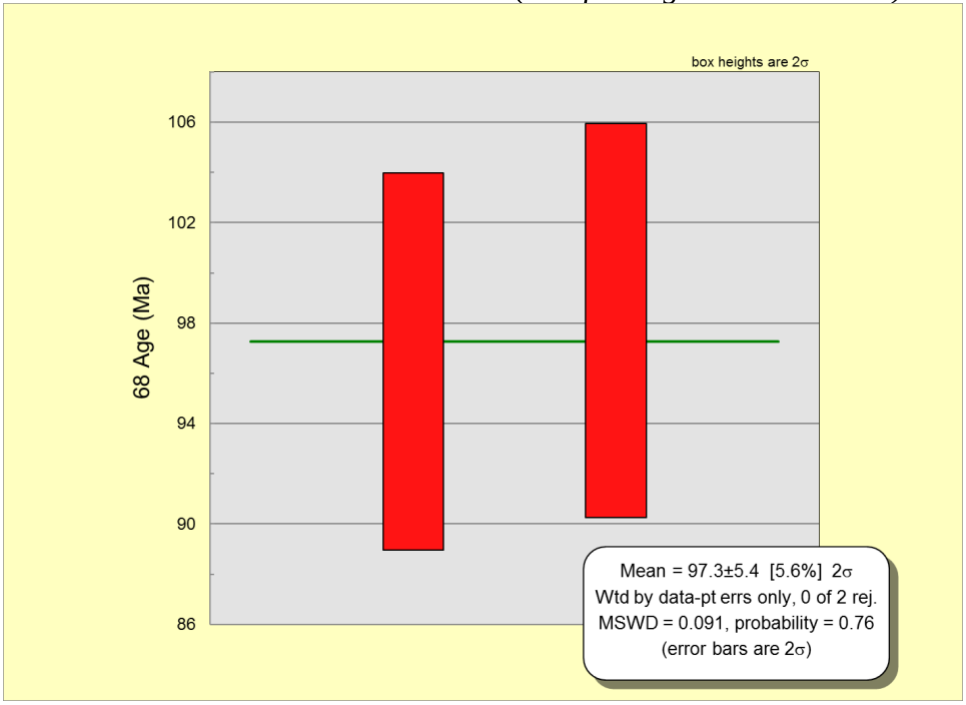

09HA12A in-mount BLR titanite std (accepted age: 1047.1 ± 0.4 Ma)

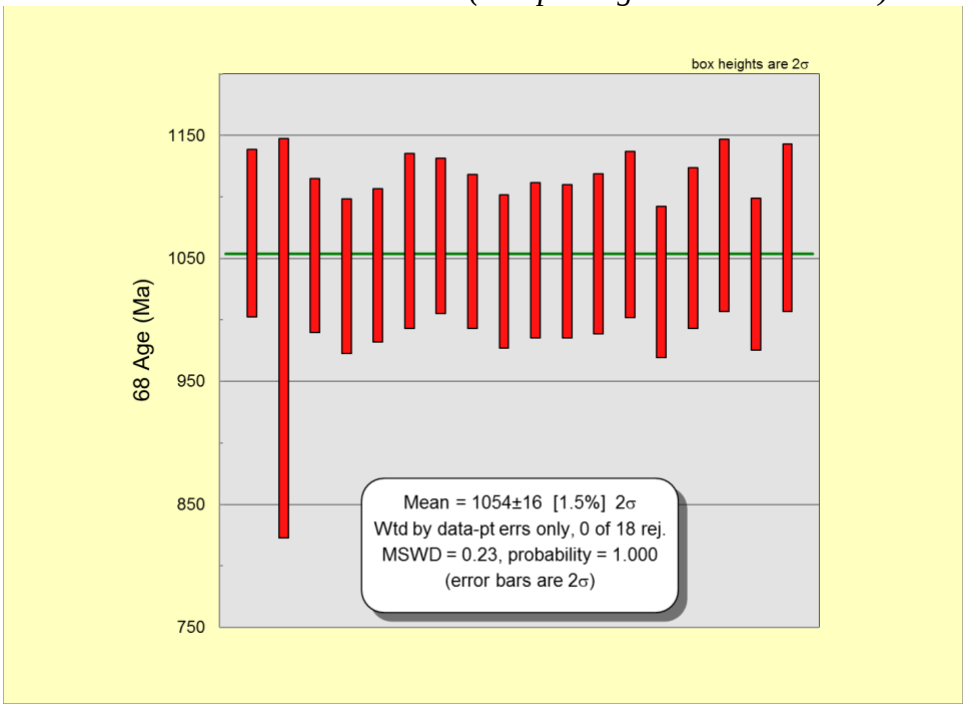

09HA12A in-mount Ecstall West zircon (accepted age: 91.5 ± 1.0 Ma)

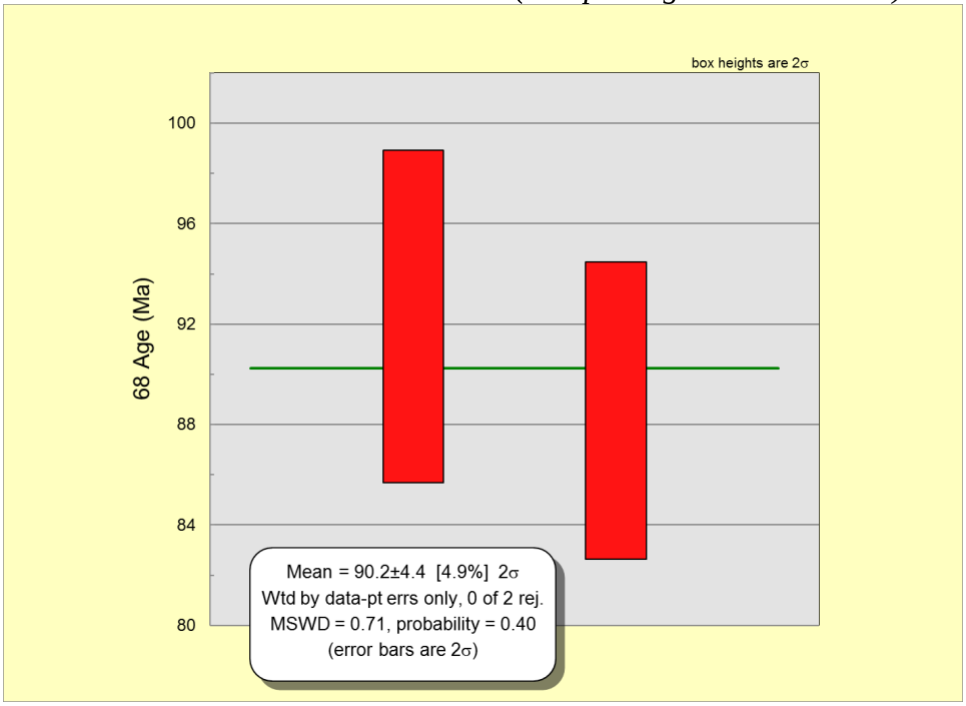

09HA12B in-mount BLR titanite std (accepted age: 1047.1 ± 0.4 Ma)

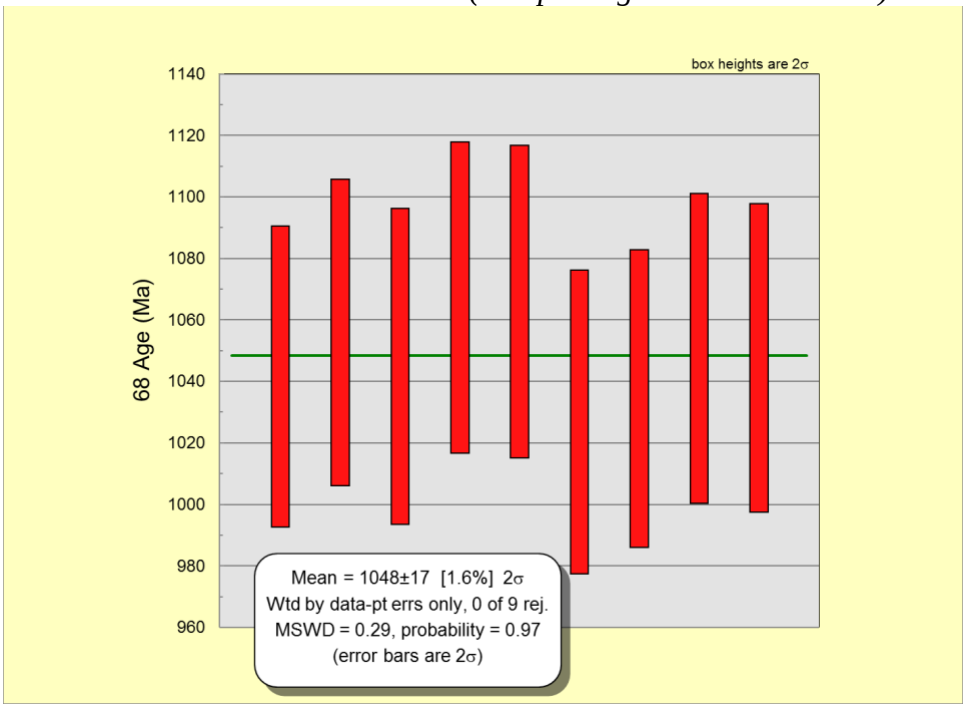

09HA12B in-mount Ecstall West zircon (accepted age: 91.5 ± 1.0 Ma)
Only one analysis: 92.5 ± 5.6 Ma (2σ)

09HA13 in-mount BLR titanite std (accepted age: 1047.1 ± 0.4 Ma)

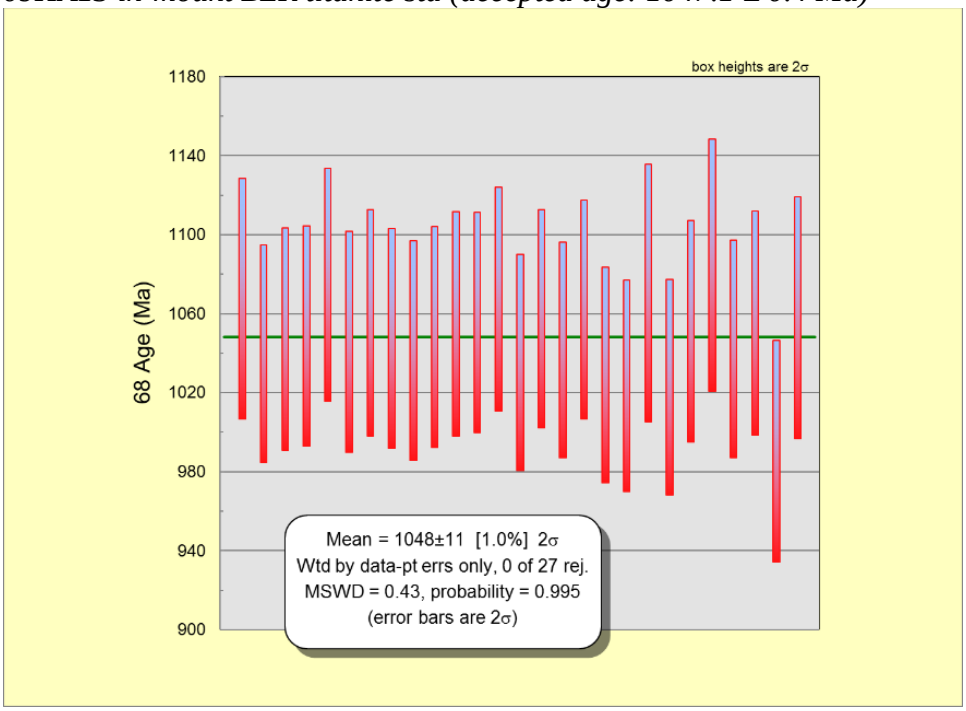

09HA13 in-mount Ecstall West zircon (accepted age: 91.5 ± 1.0 Ma)

None.

09HA18 in-mount BLR titanite std (accepted age: 1047.1 ± 0.4 Ma)

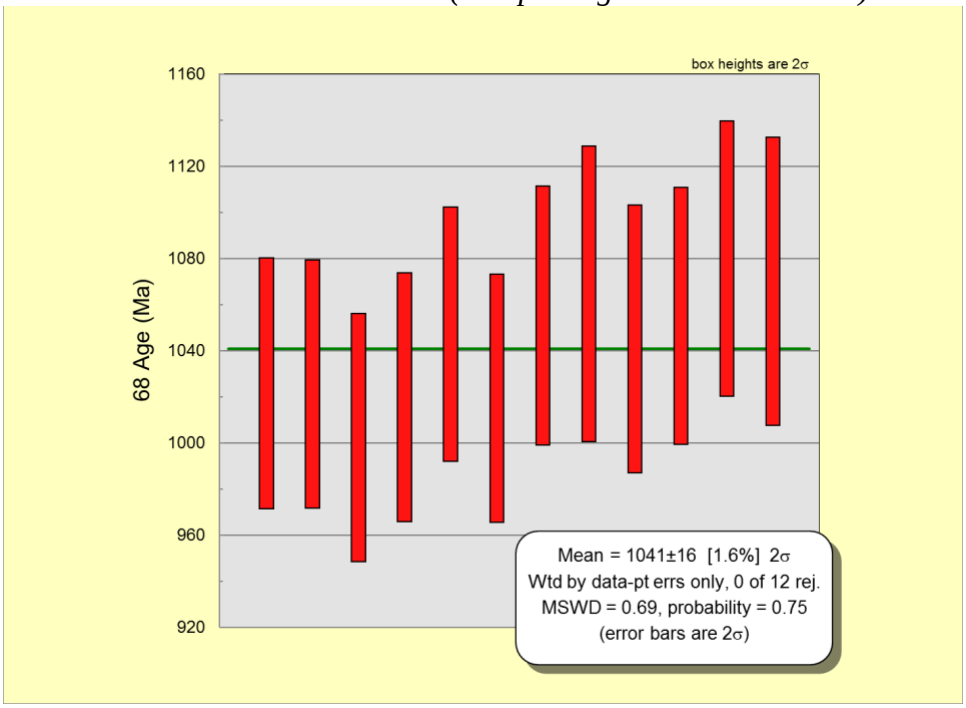

09HA18 in-mount Ecstall West zircon (accepted age: 91.5 ± 1.0 Ma)
Only one analysis: 92.1 ± 6.2 Ma (2σ)

10HA01D in-mount BLR titanite std (accepted age: 1047.1 ± 0.4 Ma)

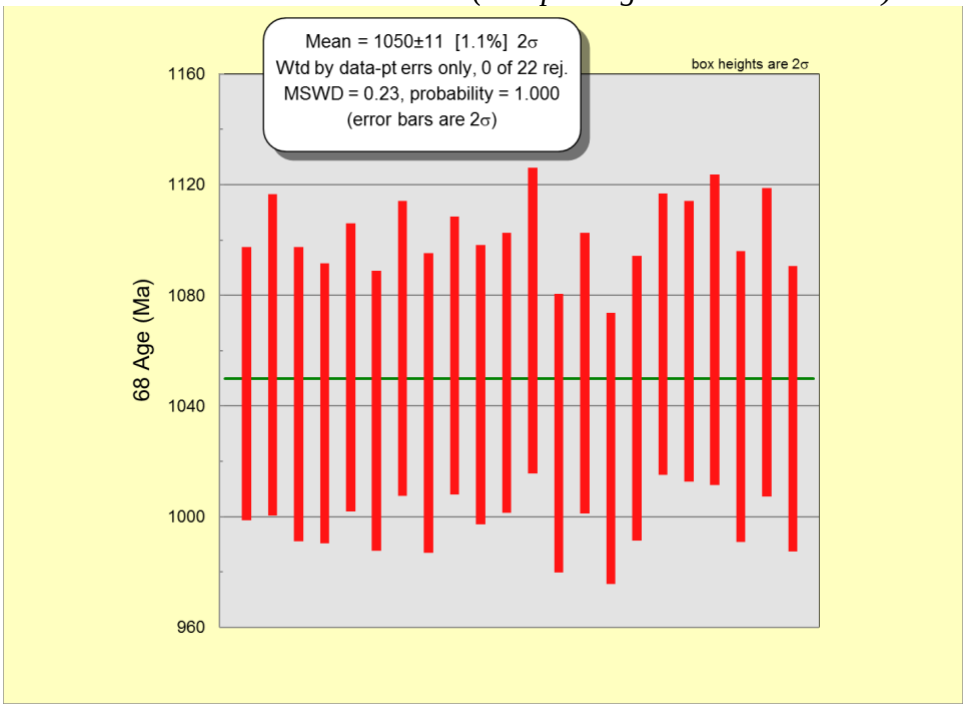

10HA01D in-mount Ecstall West zircon (accepted age: 91.5 ± 1.0 Ma)

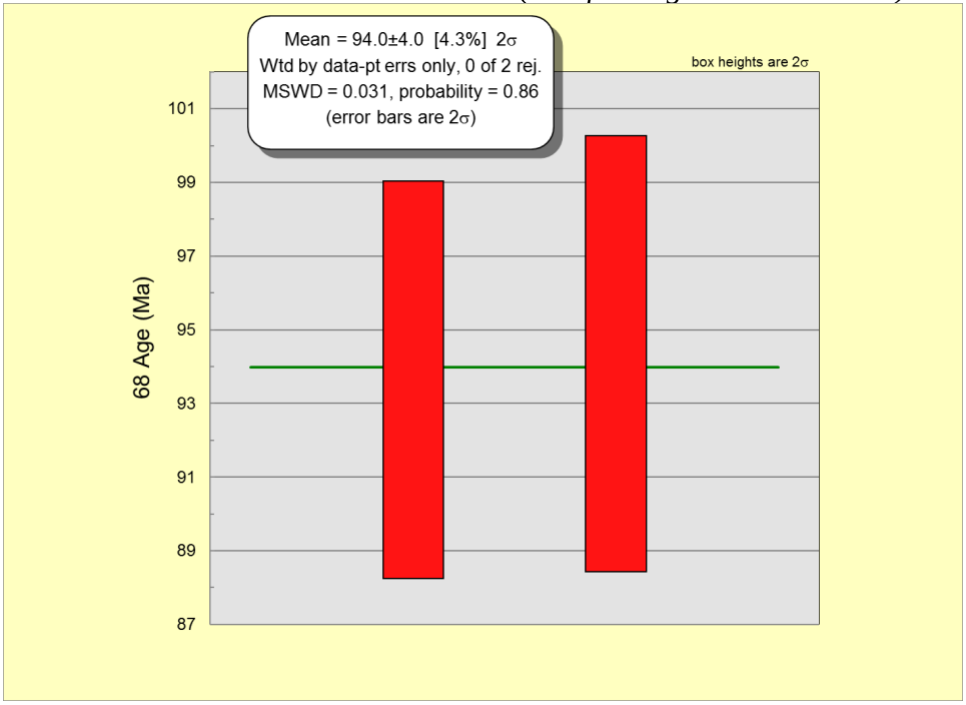

SHRIMP in-mount reference materials

Neither raw or corrected data for individual in-mount BLR analyses were provided by the ANU lab. The following information was provided with the final data table:

09HA03A: 2σ U/Pb calibration, BLR : ± 1.19%
09HA12B: 2σ U/Pb calibration, BLR : ± 0.89%
09HA13: 2σ U/Pb calibration, BLR : ± 0.62%
09HA18: 2σ U/Pb calibration, BLR : ± 0.64%

We understand these to represent the deviation of the measured U/Pb ratios in our in-mount BLR grains from the accepted U/Pb ratios in the BLR reference material. This uncertainty was propagated in quadrature for the calculation of total external uncertainties on Pb_i corrected SHRIMP dates.

As discussed in the article text, Pb isotope measurements were calibrated on the Broken Hill feldspar standard prior to SHRIMP analysis.

The same BLR grains used for calibration during SHRIMP analysis were also used during LA-ICP-MS analysis. The data from LA-ICP-MS analysis show that these grains return the expected 1047 Ma age within uncertainty, and thus we do not suspect that there is significant heterogeneity within the BLR material used that would preclude accurate SHRIMP (or LA-ICP-MS) analysis.

Supplemental Text

Tera-Wasserburg models of U-Pb evolution for titanite initially crystallized at ca. 1150 Ma

The model is a simple step-wise spreadsheet-based calculation that decays U and grows in Pb from 1150 Ma to present. Starting U abundance was chosen as 30 ppma, a typical, representative value for Harrisville titanite grains. Starting $^{235}U/^{238}U$ is 0.0189, which is back-calculated based on a modern $^{235}U/^{238}U = 1/137.82$ and 1150 Ma crystallization age. The fraction of $^{206}Pb_i$ was set at 6% (0.3 ppma) of the final radiogenic ^{206}Pb abundance, again, a typical value for the Harrisville grains. Assuming titanite crystallization from a "primordial" crustal reservoir at 1150 Ma, the Pb_i $^{207}Pb/^{206}Pb$ is 0.962, using the Stacey and Kramers (1975) two-stage crustal evolution model.

One model shows 50% Pb loss at 1050 Ma (100 m.y. after titanite crystallization), simulating Pb loss during the ca. 1050 Ma granulite facies Ottawan metamorphic event. This means that 50% of all Pb (on an atomic basis) accumulated over the first 100 m.y. was subtracted from the model at the 100 m.y. time step, then the remaining U was allowed to decay as before and radiogenic Pb to grow in for an additional 1050 m.y., adding to the reduced pool of pre-loss Pb. For the other model, 50% of all Pb was lost at 550 Ma (~600 m.y. after titanite crystallization) to simulate a much more recent Pb loss event. In this case, 50% of all Pb (on an atomic basis) accumulated over the first 600 m.y. was subtracted from the model at this time step, then the remaining U was allowed to decay as before and Pb to grow in, adding to the reduced pool of pre-loss Pb.

The $^{207}Pb/^{206}Pb$ ratio at each time step is calculated as the sum of the atoms of $^{207}Pb_i$ and $^{207}Pb^*$ divided by the sum of the atoms of $^{206}Pb_i$ and $^{206}Pb^*$. The $^{238}U/^{206}Pb$ ratio at each time step is calculated as the ^{238}U divided by the sum of the atoms of $^{206}Pb_i$ and $^{206}Pb^*$.

American Mineralogist: November 2020 Deposit AM-20-117274

Supplemental Figures S1-S13

Supplemental Figures S1-S13 show traverse data for the Adirondack titanite grains described in this study. Figures include grain images that indicate chemical zoning and the locations of various analyses, especially U-Pb analyses. Unless otherwise noted, grain images are SEM BSE; some of which are adjusted for high contrast to bring out subtle chemical zoning. Note that in several images, U-Pb SIMS analyses appear as large black areas but the actual pit sizes are smaller than the dark areas, which show pre-analysis beam rastering and removal of carbon coat ("burn marks").

Traverse data are displayed in three panels. The uppermost shows $^{238}U/^{206}Pb$ date uncorrected Pb_i (dotted line) and $^{238}U/^{206}Pb$ dates corrected for Pb_i (solid line). The middle panel shows $^{204}Pb/^{206}Pb$ uncorrected for Pb_i. The lowermost panel shows Th/U ratio, an indicator of chemical (specifically, growth or recrystallization) zoning.

For each figure: Circled numbers indicate the starting points of data traverses at grain edges. Vertical bars indicate the average ±1σ uncertainty for individually corrected dates and gray dashed lines show mean concordia-intercept age from 3D linear isochron regressions of all data for the given grain. Uncertainties for concordia-intercept ages are not shown and are commonly large (see Figs. 3,4).

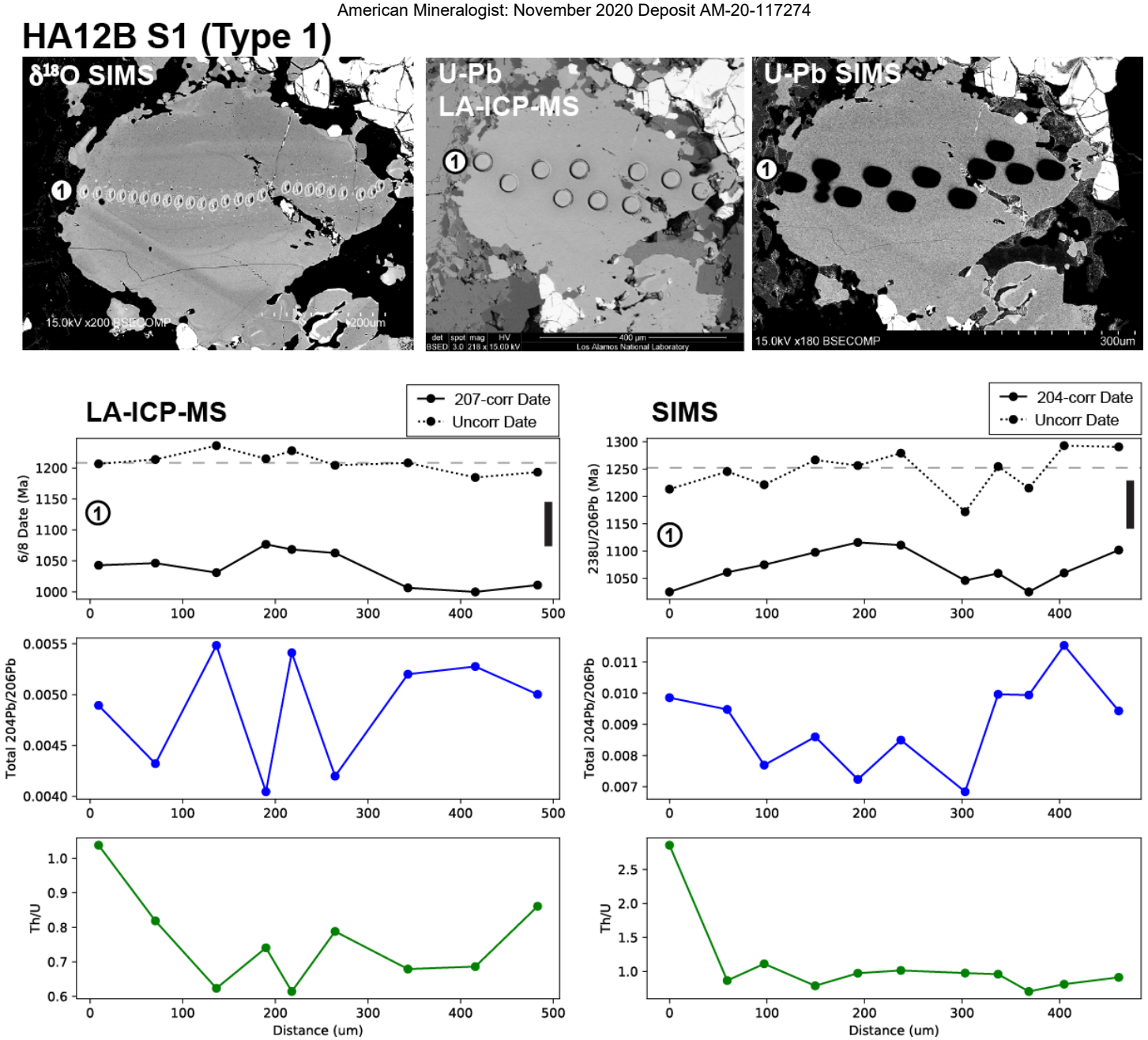

Figure S1. BSE images of grain HA12B S1. Left image taken with high contrast to visualize subtle interior compositional zoning in the grain.

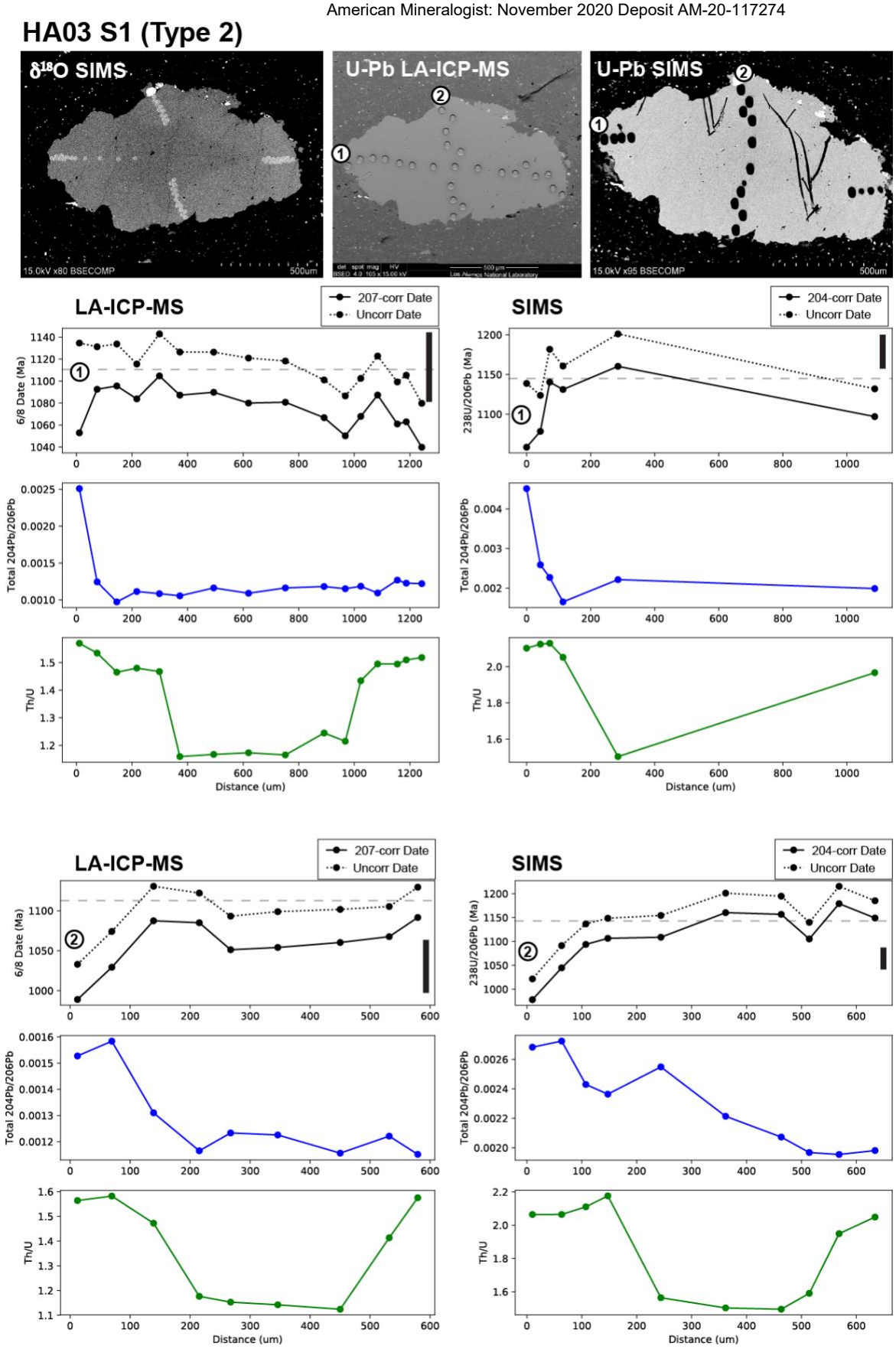

Figure S2. BSE images of grain HA03. Left image taken with high contrast to visualize subtle interior compositional zoning in the grain.

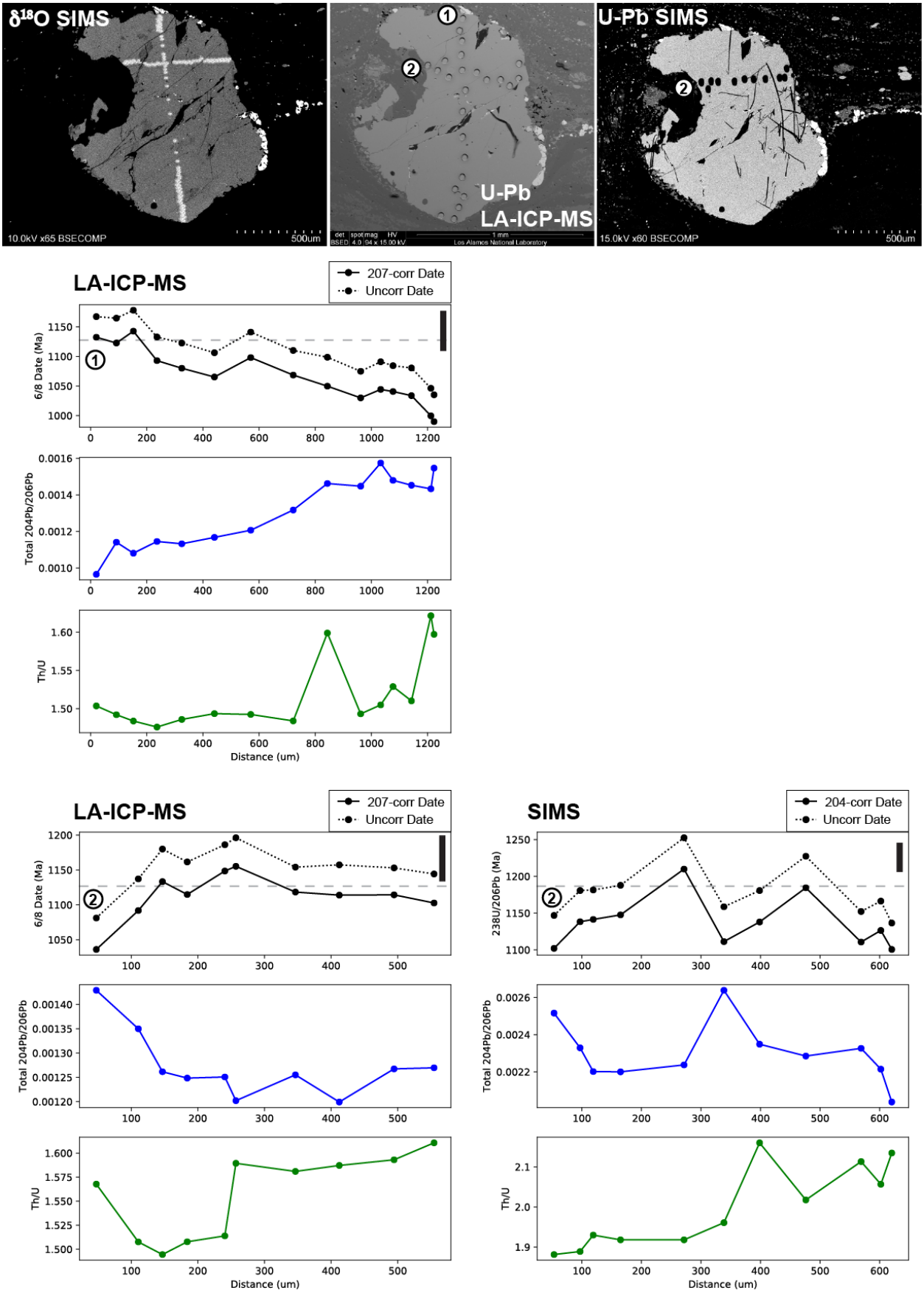

Figure S3. BSE images of grain HA03 S2. Left and right image taken with high contrast to visualize subtle interior compositional zoning in the grain.

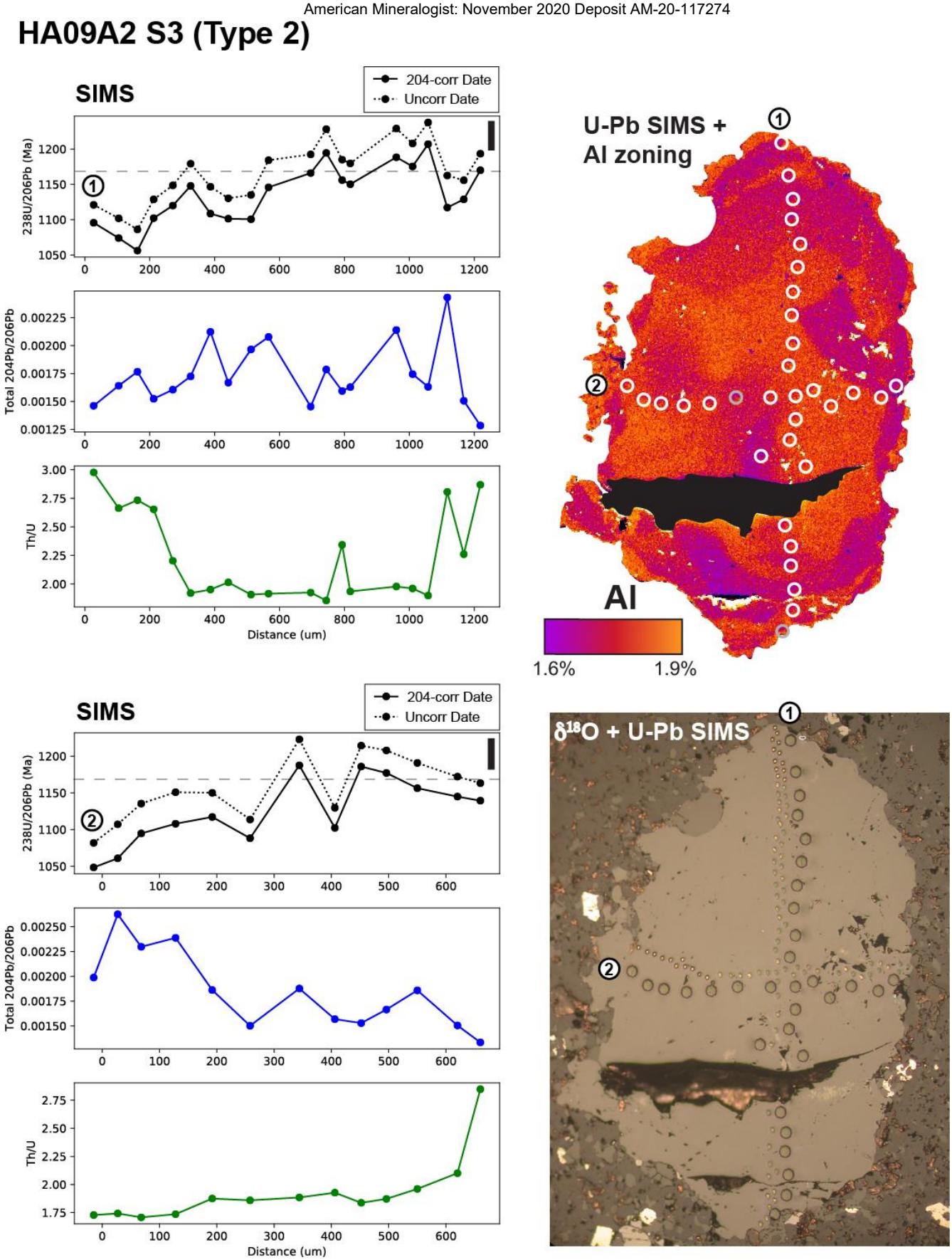

Figure S4. EMPA Al map (upper right) and reflected light image (lower right) of grain HA09A2 S3. Larger pits in lower image are from U-Pb SHRIMP analysis; smaller pits are from $\delta_{18}O$ SIMS analysis.

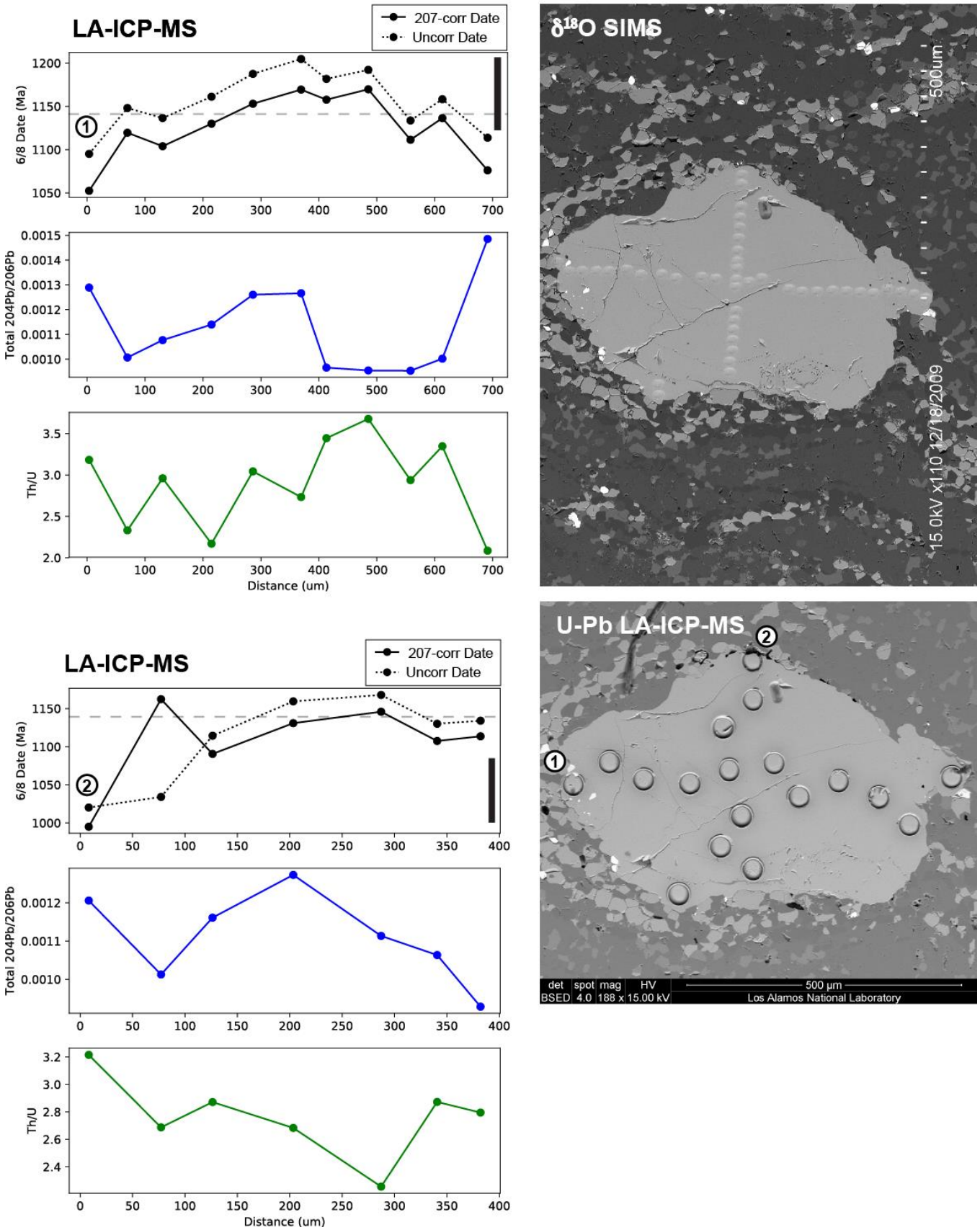

Figure S5. BSE images of grain HA09A S2.

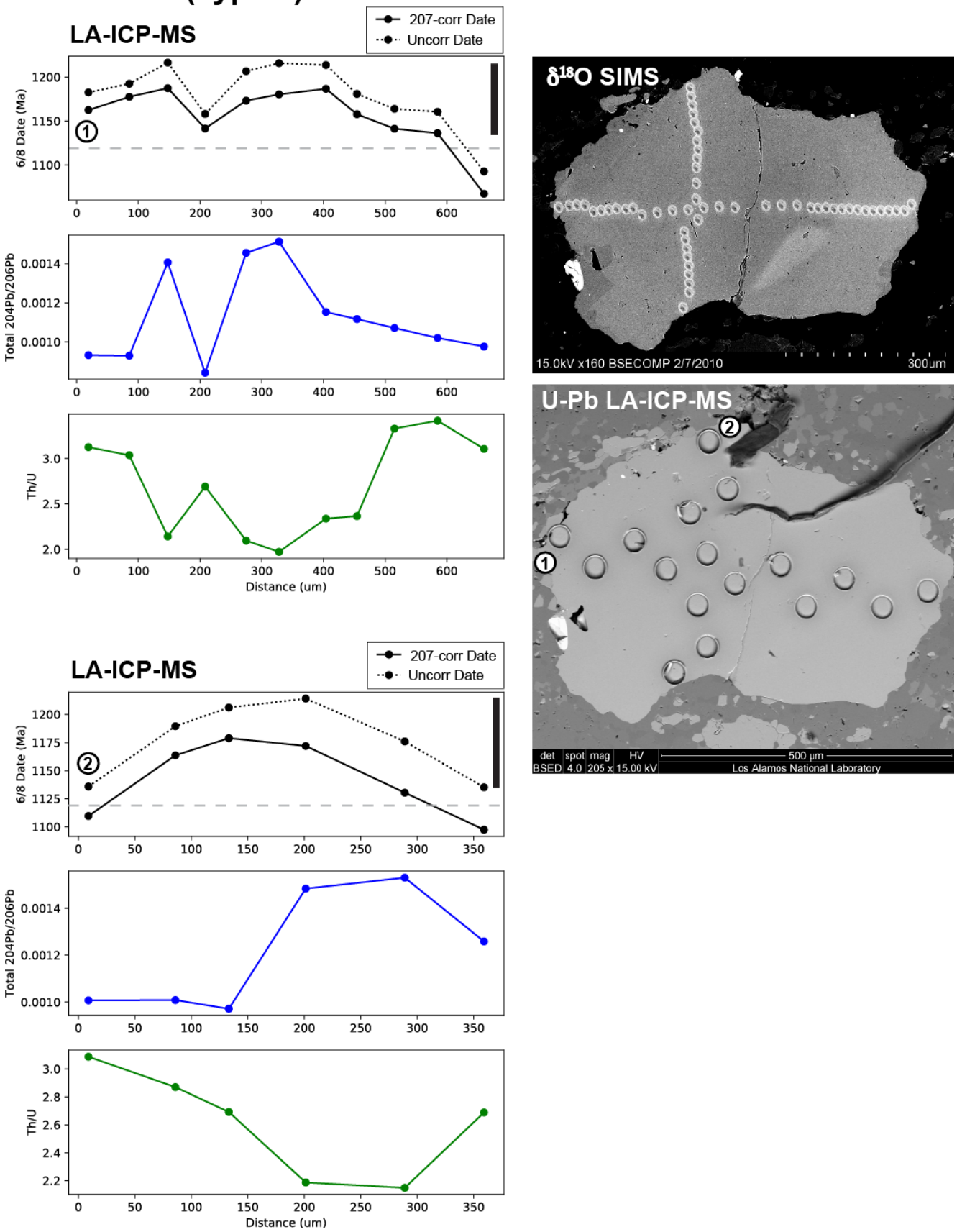

Figure S6. BSE images of grain HA09A S15. Upper image taken with high contrast to visualize subtle interior compositional zoning in the grain.

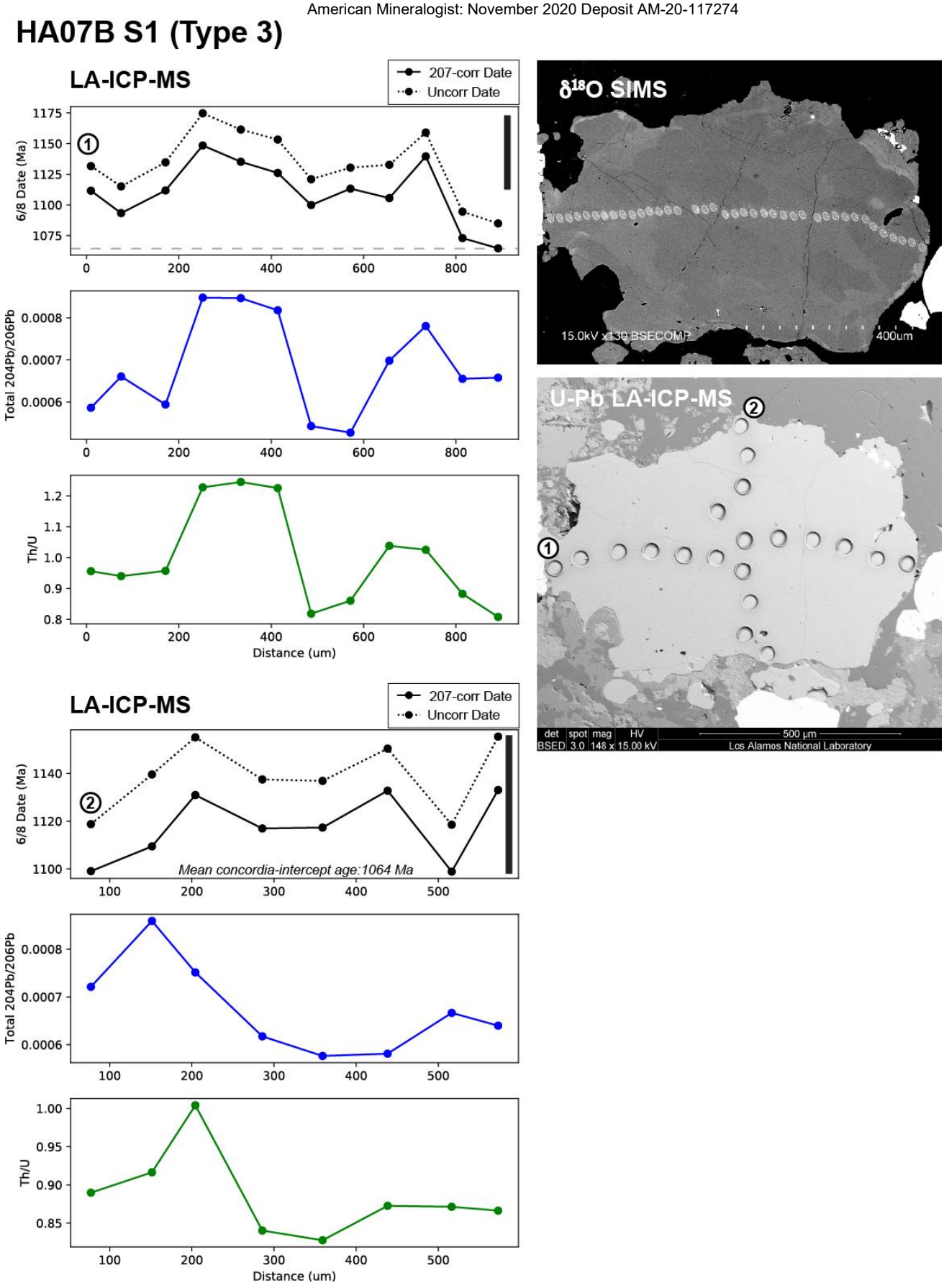

Figure S7. BSE images of grain HA07B S1. Upper image taken with high contrast to visualize subtle interior compositional zoning in the grain.

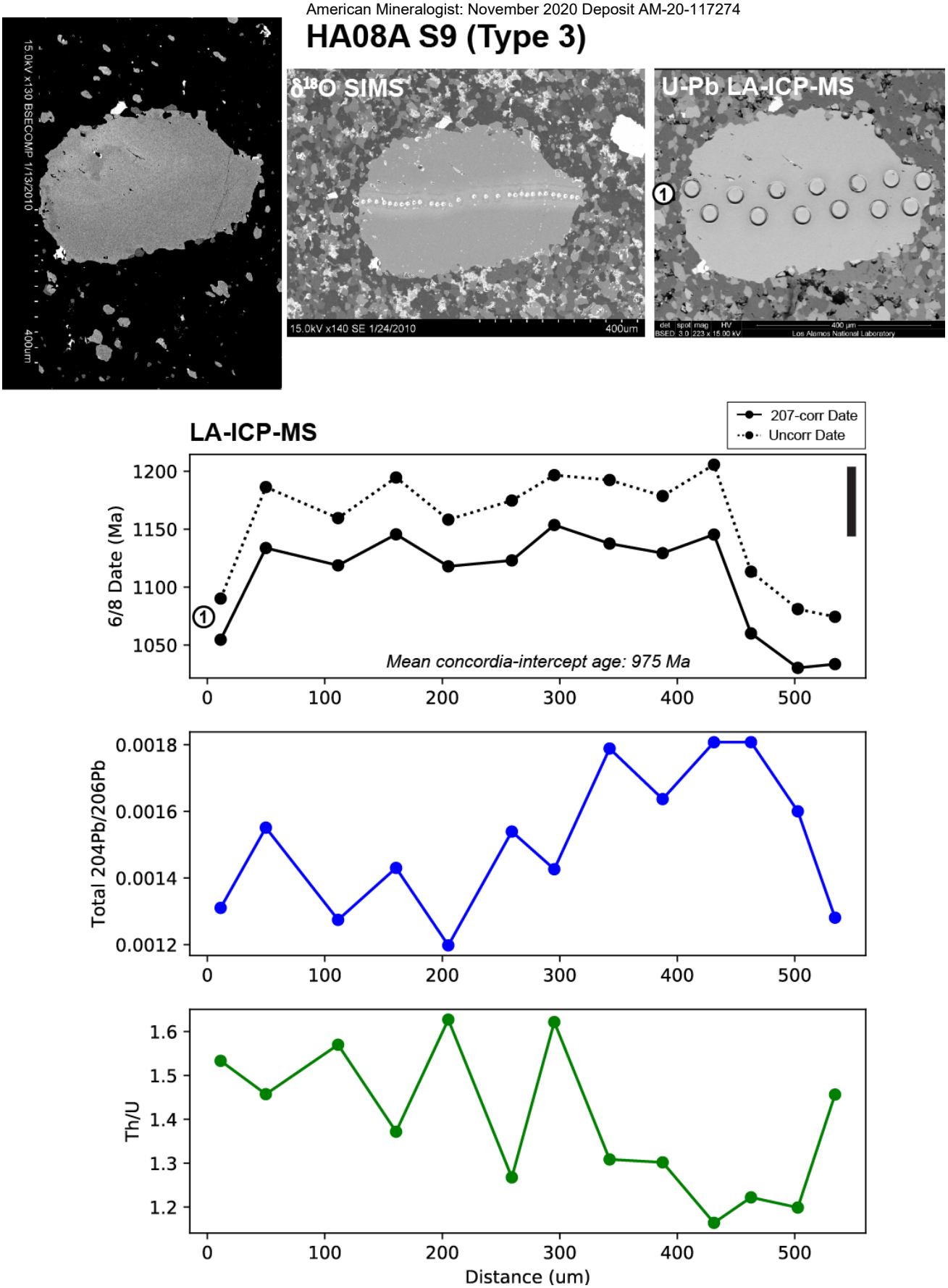

Figure S8. BSE images of grain HA08A S9. Left image taken with high contrast to visualize subtle interior compositional zoning in the grain.

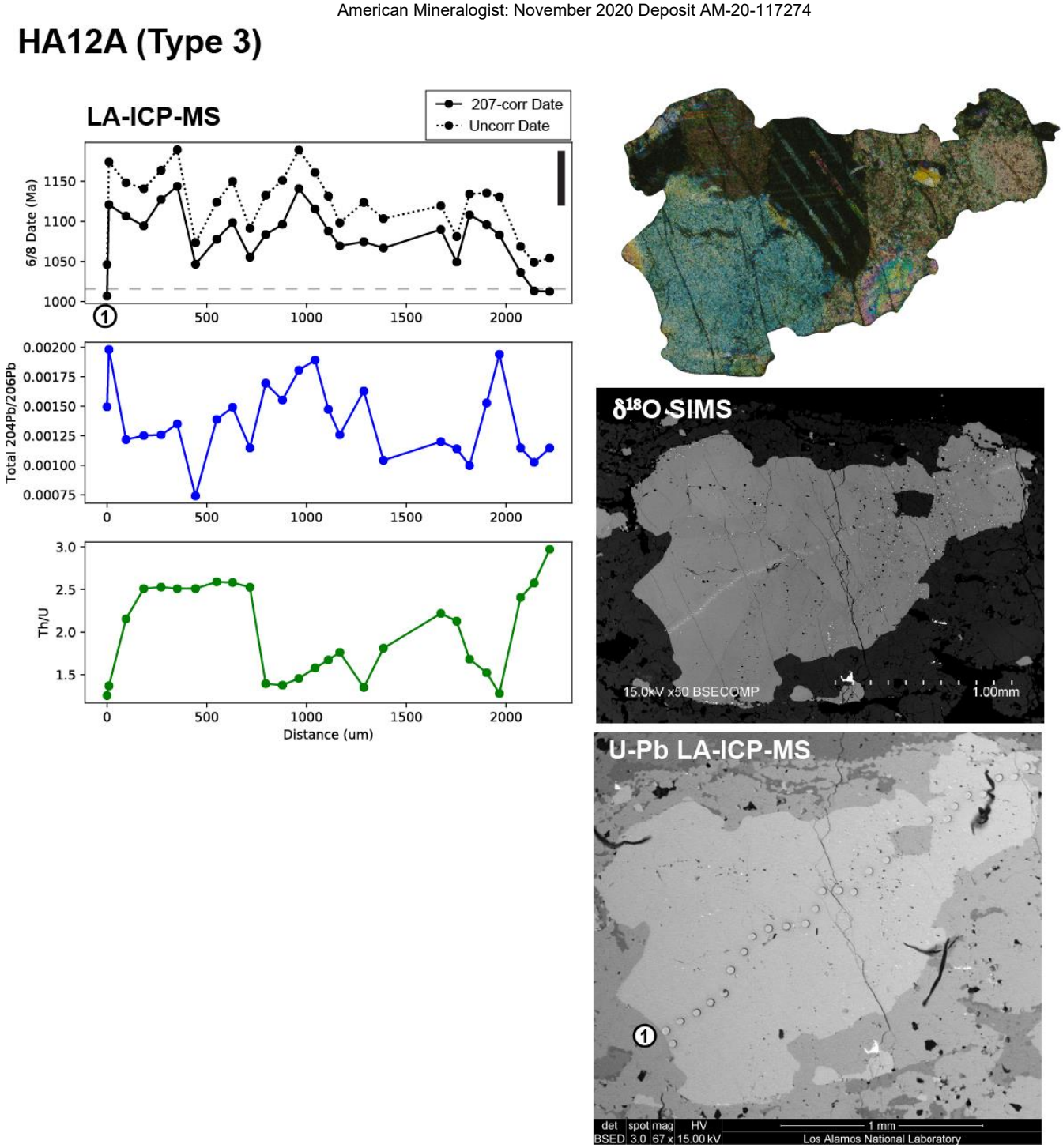

Figure S9. Cross-polarized transmitted light image (upper) and BSE images (center, bottom) of grain HA12A.

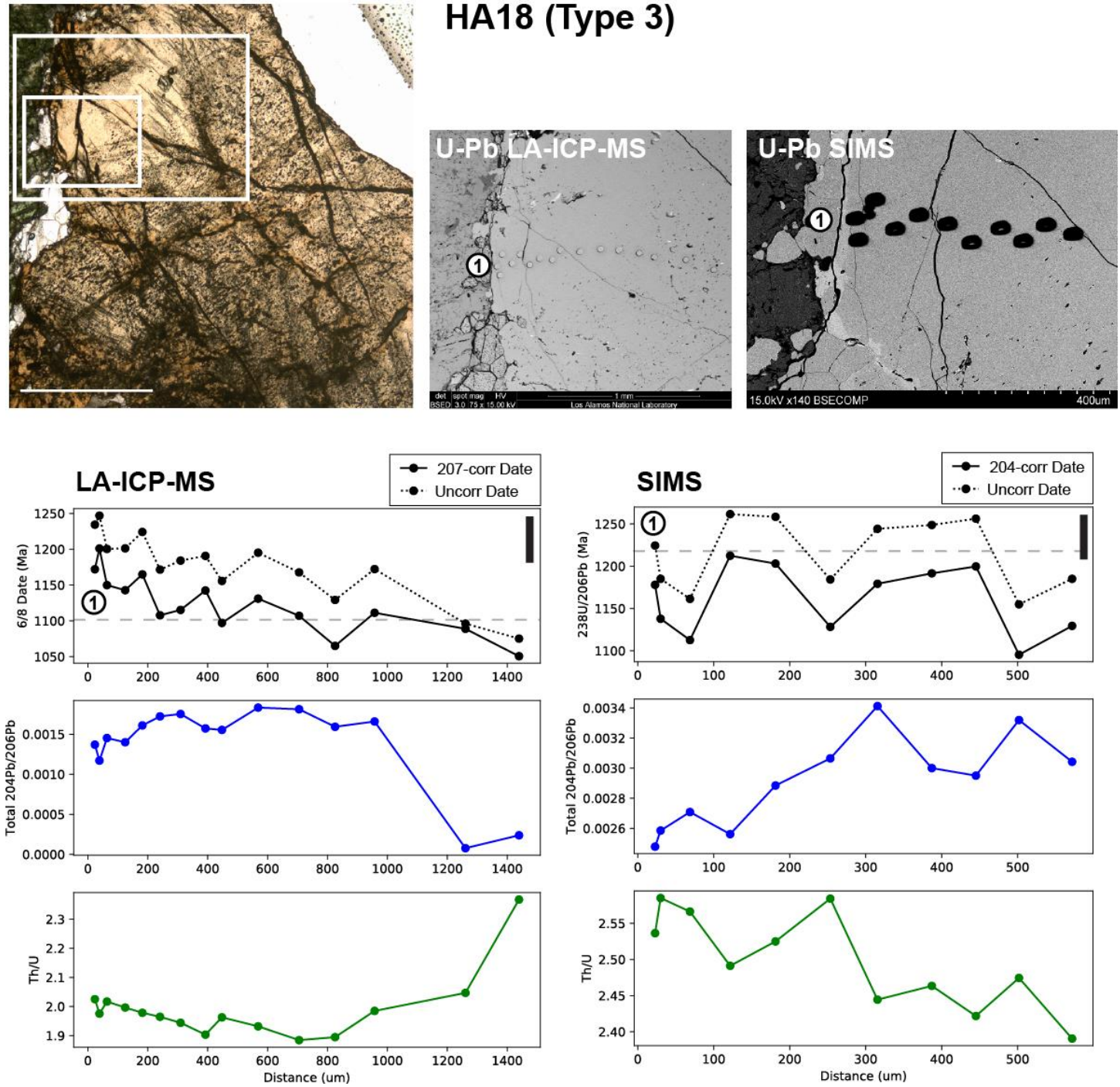

Figure S10. Plane-polarized transmitted light image (left), SE image (center), and BSE image (right) of HA18. White boxes in left image indicate areas shown in the adjacent SEM images.

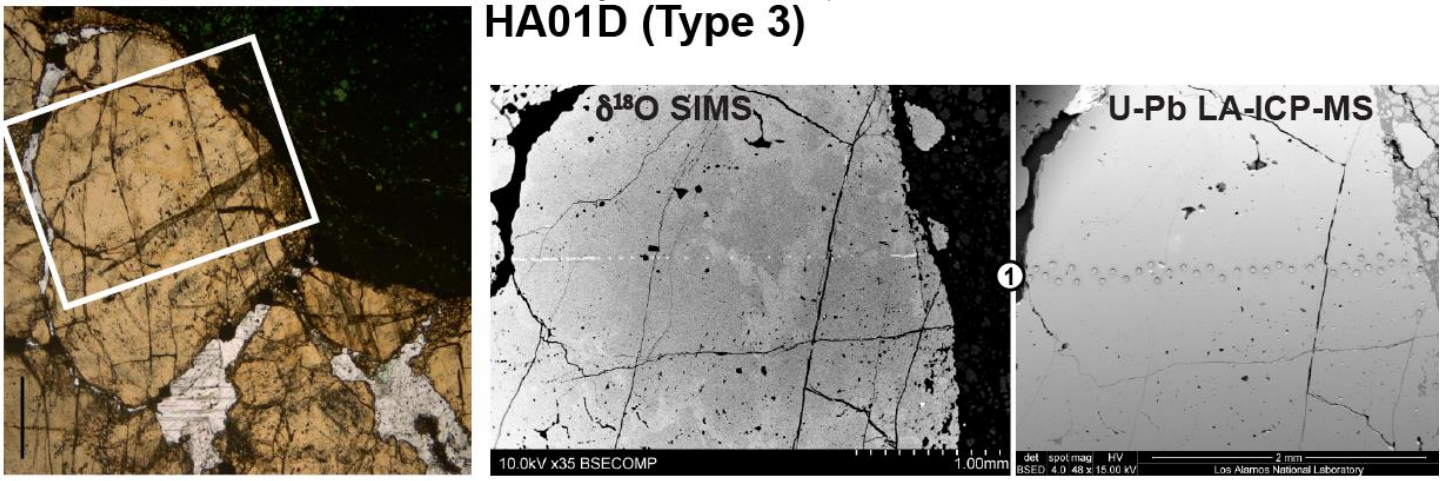

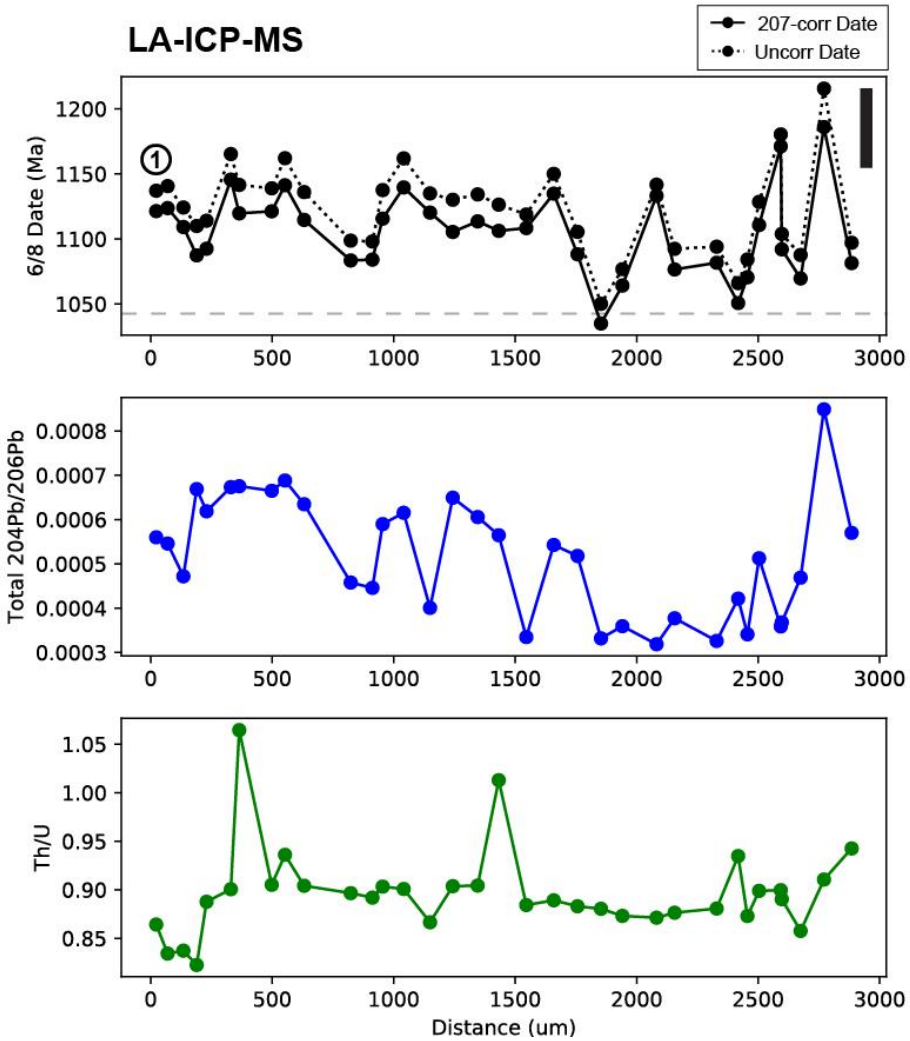

Figure S11. Plane-polarized transmitted light image (left) and BSE images (center, right) of grain HA01D. White box in left image indicates area shown in the adjacent SEM BSE images.

HA13 S1 (Type 4)

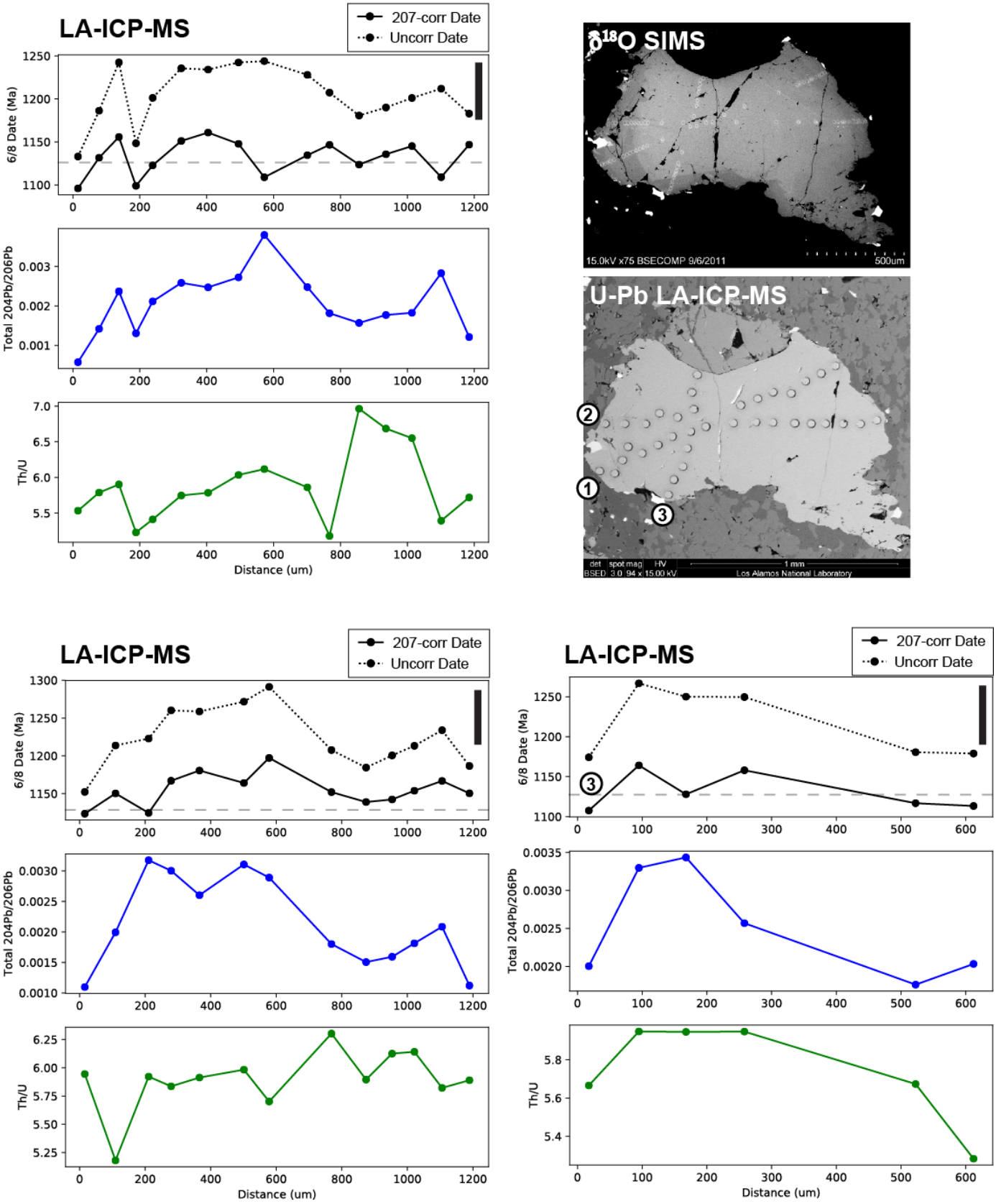

Figure S12. BSE images of grain HA13 S1. Upper image taken with high contrast to visualize subtle interior compositional zoning in the grain.

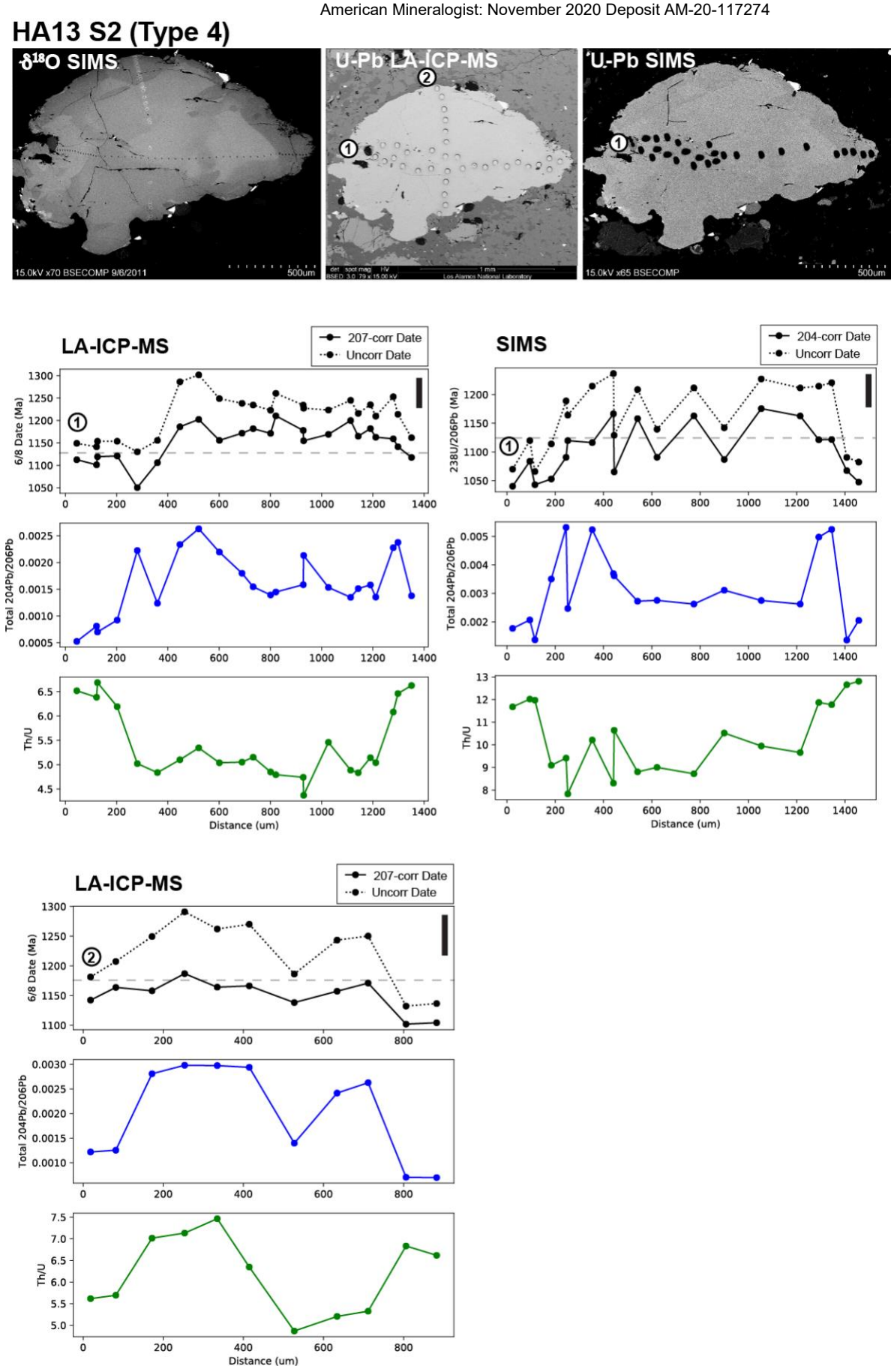

Figure S13. BSE images of grain HA13 S2. Left image taken with high contrast to visualize subtle interior compositional zoning in the grain.